THE JOURNAL OF BIOLOGICAL CHEMISTRY VOL. 287, NO. 17, pp. 13598–13610, April 20, 2012

Insights into Mechanism of Glucokinase Activation

OBSERVATION OF MULTIPLE DISTINCT PROTEIN CONFORMATIONS[S]

Received for publication, June 20, 2011, and in revised form, January 30, 2012 Published, JBC Papers in Press, February 1, 2012, DOI 10.1074/jbc.M111.274126

Shenping Liu[‡1], **Mark J. Ammirati**[‡], **Xi Song**[‡], **John D. Knafels**[‡], **Jeff Zhang**[‡], **Samantha E. Greasley**[§], **Jeffrey A. Pfefferkorn**[¶], **and Xiayang Qiu**[‡]

From the [‡]*Structural Biology and Biophysics and* [¶]*Cardiovascular Metabolic and Endocrine Disease Research, Pfizer Groton Laboratories, Groton, Connecticut 06340 and* [§]*Structural Biology and Biophysics, Pfizer La Jolla Laboratories, San Diego, California 92121*

Background: Human glucokinase (GK) is a principal regulator of glucose homeostasis.
Results: The structure of the catalytic complex of GK has been determined, and multiple conformations have been directly observed in solution.
Conclusion: In solution, glucose dose-dependently converts GK from the apo conformation to an active open conformation.
Significance: Understanding the conformational changes of GK during the reaction is crucial for designing better glucokinase activators with safer profiles.

Human glucokinase (GK) is a principal regulating sensor of plasma glucose levels. Mutations that inactivate GK are linked to diabetes, and mutations that activate it are associated with hypoglycemia. Unique kinetic properties equip GK for its regulatory role: although it has weak basal affinity for glucose, positive cooperativity in its binding of glucose causes a rapid increase in catalytic activity when plasma glucose concentrations rise above euglycemic levels. In clinical trials, small molecule GK activators (GKAs) have been efficacious in lowering plasma glucose and enhancing glucose-stimulated insulin secretion, but they carry a risk of overly activating GK and causing hypoglycemia. The theoretical models proposed to date attribute the positive cooperativity of GK to the existence of distinct protein conformations that interconvert slowly and exhibit different affinities for glucose. Here we report the respective crystal structures of the catalytic complex of GK and of a GK-glucose complex in a wide open conformation. To assess conformations of GK in solution, we also carried out small angle x-ray scattering experiments. The results showed that glucose dose-dependently converts GK from an apo conformation to an active open conformation. Compared with wild type GK, activating mutants required notably lower concentrations of glucose to be converted to the active open conformation. GKAs decreased the level of glucose required for GK activation, and different compounds demonstrated distinct activation profiles. These results lead us to propose a modified mnemonic model to explain cooperativity in GK. Our findings may offer new approaches for designing GKAs with reduced hypoglycemic risk.

Human glucokinase (GK[2]; hexokinase 4; hexokinase D) (EC 2.7.1.2) catalyzes the conversion of glucose to glucose 6-phosphate and is a principal regulator of glucose homeostasis (1, 2). In non-hepatic tissues, such as β-islets, brain, and gut, GK expression is driven by one of the GK gene promoters (3). Transcription of the GK gene in the liver of diabetic rats is induced by insulin (4). Entry of glucose to hepatocytes and β-islets is fast and unrestricted, and GK is the predominant enzyme that catalyzes the phosphorylation of glucose in both tissues. In pancreatic β-islets, GK provides a concentration-dependent adjustment of the rate of the initial reaction of glucose metabolism that directly controls glucose-stimulated insulin secretion (GSIS) through the entire glycolysis and glucose oxidation pathways (5). In hepatocytes, short term regulation of GK activity occurs through its interaction with a liver-specific GK regulatory protein (GKRP). At low glucose concentrations, GK is sequestered in the nucleus through its binding with GKRP, but when the glucose concentration increases, GK dissociates from GKRP and is transported into the cytoplasm to facilitate the uptake of glucose and its conversion into glycogen (6). Enhanced GK expression in the liver after insulin stimulation provides long term up-regulation of GK activity (4).

GK differs from other hexokinases in that it has much lower glucose affinity (half-saturating concentration ($S_{0.5}$), 7–8 mM), has positive cooperativity (Hill coefficient, 1.7), and is not affected by product inhibition (2). These properties of GK equip it perfectly for its role in glucose homeostasis, and its importance is highlighted by the clinical impact of GK variants. Mutants with decreased enzyme activity are associated with hyperglycemia and maturity onset diabetes of the young type 2 (7–10), whereas activating mutations result in hypoglycemia and hyperinsulinemia with symptoms ranging from mild to

[S] This article contains a supplemental movie.
The atomic coordinates and structure factors (codes 3VEV, 4DHY, 3VF6, 3VEY, and 4DCH) have been deposited in the Protein Data Bank, Research Collaboratory for Structural Bioinformatics, Rutgers University, New Brunswick, NJ (http://www.rcsb.org/).

[1] To whom correspondence should be addressed: Structural Biology and Biophysics, Pfizer Groton Laboratories, Eastern Point Rd., Groton, CT 06340. Tel.: 860-686-6959; Fax: 860-686-2095; E-mail: shenping.liu@pfizer.com.

[2] The abbreviations used are: GK, glucokinase; GSIS, glucose-stimulated insulin secretion; SAXS, small angle x-ray scattering; GKA, glucokinase activator; GKRP, GK regulatory protein; ATPγS, adenosine 5′-*O*-(thiotriphosphate); Bis-Tris, 2-[bis(2-hydroxyethyl)amino]-2-(hydroxymethyl)-propane-1,3-diol; CCD, charge-coupled device; AMPPNP, adenosine 5′-(β,γ-imino)triphosphate.

severe depending on the degrees to which these activating mutations lower $S_{0.5}$ and diminish the cooperativity of the reaction (11, 12).

Because GK contributes so critically to glucose homeostasis, small molecule allosteric activators of GK have been actively sought as treatments for diabetes. Numerous GK agonists (GKAs) showing efficacy in enhancing GSIS and lowering plasma glucose have entered clinical trials as treatments for type 2 diabetes mellitus (13–22), but their efficacy has been accompanied by a major element of hypoglycemic risk that narrowed the therapeutic window. As with severely activating mutations of GK, the hypoglycemia observed with earlier GKAs resulted from a greatly reduced dependence of GK activity on glucose concentrations ($S_{0.5} < 1$ mM) in the presence of these compounds (full GK agonists), resulting in fully activated liver GK and greatly stimulated GSIS (13–17). For this reason, such compounds have been termed full GK agonists. To avoid the hypoglycemic risk, current efforts on GKAs focus on compounds that either lower $S_{0.5}$ more moderately (partial GK agonists) (18, 19) or selectively target hepatocytes (hepatoselective GK agonists) (20, 21). Hepatoselective GKAs would fully activate GK in the short term by dissociating GK from GKRP at low glucose concentrations but would avoid long term GK activation caused by up-regulated GK expression induced by stimulation of GSIS (20, 21). Ideal GKAs will mimic mild GK-activating mutations that lower the glucose level with minimal hypoglycemic risk. An understanding of the activation mechanism of GK will help in designing GKAs with better safety profiles.

Positive substrate cooperativity causes GK activity to exhibit a sigmoidal response to glucose concentration with an inflection point at 5 mM (euglycemia), consistent with its role in sensing glucose (2). Most unusually for an allosteric enzyme, GK is a monomeric protein with a single active site. Two earlier models have been proposed to explain its cooperativity: a mnemonic model and a slow transition model (23, 24). Both predict the existence of two distinct conformations of the enzyme that interconvert slowly and have different affinities for glucose (25–31). In the mnemonic model, the predominant conformation at low glucose concentration (<5 mM) has low affinity for glucose but is converted by glucose in a dose-dependent manner to a high affinity conformation (23). In the slow transition model, the cooperativity of GK stems mainly from the kinetic behavior of the enzyme: if GK could reach equilibrium during the catalytic reaction, the majority of GK molecules would adopt the high affinity conformation even at low glucose concentration (<5 mM) (24). Both models predict that the conversion between the two conformations is slower than the reaction cycle. The mnemonic model also predicts that the percentage of molecules in the high affinity state determines the level of GK activity. In contrast, the slow transition model predicts that the low and high affinity species participate in two different reaction cycles (31). Because the biochemical assays only gauge production of the final product, it has been difficult to determine which model is correct by traditional methods.

Recent studies, including x-ray crystallography (13–22), stopped-flow kinetic studies, equilibrium and pre-steady-state fluorescent spectroscopic studies, and high resolution NMR, support the idea that GK is an intrinsically mobile protein that can sample many different conformational states with different glucose affinities (26–32). In reported crystal structures of both apoGK (14) and numerous glucose-GKA complexes (13–22), the overall structure of GK has been found to consist of two domains. The small domain is composed of residues 66–202 and helix C, which consists of residues 442–465 (the C terminus). The large domain accounts for the rest of the protein (see Fig. 1). In most structures of GK complexes, the enzyme adopts an active closed conformation in which glucose is completely buried at a binding site formed by residues from both domains (13–15, 17–22). In this active closed conformation, glucose forms extensive interactions with GK, and all its hydroxyl groups have hydrogen bond partners. In the apoGK structure, the binding site for glucose is not completely formed (14), and this has been postulated to represent the low affinity conformation of GK. In this conformation, all the key glucose-interacting residues from the small domain are far away from the glucose binding site (14).

The large domain remains essentially unchanged in these two different conformations, but the small domain undergoes a large conformational change when switching between them. Not only is there a rigid body motion of the small domain relative to the large domain, but large scale secondary structure rearrangements also occur (14). These require disruption and reformation of numerous interactions in the small domain and have been proposed as the structural basis for the slow transition rate from the apo conformation to the active closed conformation (14). It was suggested that this conformational change is slower than the reaction cycle, which involves chemical turnover and perhaps a simple rigid body motion that converts GK between the active closed conformation and a yet to be observed active open conformation (14). This active open conformation of GK was suggested, based on kinetic analysis and modeling, to be required for the release of the reaction products and binding of new substrates (14, 33). In fact, both the active closed and active open conformations have been observed in crystal structures of other hexokinases (34, 35).

To further our understanding of the catalytic mechanism of GK, we have determined the crystal structure of the catalytic complex of GK with a non-hydrolyzable ATP analog, ATPγS, and demonstrated that the catalytic complex adopts the active closed conformation. We also report the crystal structure of a glucose-GK complex with a conformation distinct from either the active closed conformation or the apo conformation. In this conformation, all the glucose-interacting residues from the small domain are far away from glucose. We call this state of the enzyme the active wide open conformation and propose that it is similar to but not exactly the same as the active open conformation expected to exist in the reaction cycle.

The apo and the glucose-bound GK crystal structures would support the mnemonic model of GK cooperativity were it not for the fact that all the glucose-bound GK crystals were obtained in the presence of very high concentration of glucose (Refs. 13–22; also see "Experimental Procedures") and (in almost every case) in the presence of a GKA. Such compounds greatly increase the affinity of glucose for GK (13–22). To gain more insight into the mechanism of positive cooperativity, it

would be desirable to achieve direct observations of GK conformation in solution, especially at physiologically relevant glucose concentrations. In addition, because of crystal lattice constraints, the conformations observed in crystals may not represent the dominant species in solution and are unlikely to reveal all the steps required for the catalytic reaction (14, 26–32). Indeed, many intermediate conformational states of GK have been observed in pre-steady-state fluorescence spectroscopic studies (27–29).

SAXS can provide the size, overall shape, and global conformation of a macromolecule in solution under physiological conditions (36–40). In combination with crystallography, SAXS can link the global conformation of an enzyme in solution directly with its catalytic mechanism at the atomic level. In addition to our crystallographic studies, we report here the results of our SAXS studies of the effects of various ligands, including glucose, nucleotides, and GKAs, on the solution conformations of wild type GK and two activating mutants. These studies confirm that in the absence of glucose GK mainly adopts the apo conformation observed in crystals. Glucose dose-dependently induces a glucose-bound GK conformation different from either the active closed conformation or the active wide open conformation observed in crystals. This glucose-bound conformation is more compact than the apo conformation. We constructed an active open conformation model by fitting SAXS curves with conformations generated by morphing between the active closed and the active wide open conformations. Activating GK mutations and GKAs were found to lower the glucose concentration at which GK is converted to the active open conformation, providing a structural rationale for their related effects on GK activation.

Our crystallographic and SAXS results lead us to favor a modified mnemonic model to describe cooperativity in GK. It predicts that at low glucose concentration the predominant conformation of GK in solution is the apo conformation, that there is only one major reaction cycle, and that it involves both the active open and active closed conformations. The application of SAXS to studying the effects of small molecule GKAs on GK conformation has provided a unique opportunity to further understand the structural, conformational, and functional attributes of these emerging therapeutic agents.

EXPERIMENTAL PROCEDURES

Protein Expression and Purification—Wild type GK protein used for crystal soaking of the active closed conformation crystal form, SAXS experiments, and co-crystallization of the active wide open conformation crystal form was expressed and purified according to reported protocols (13, 14). The activating mutants of GK used in SAXS experiments (T65I and Y214S) were obtained using the QuikChange® Lightning site-directed mutagenesis kit (Stratagene, La Jolla, CA). Activating mutants were expressed under the same conditions as the wild type GK. N-His-tagged GK was purified by immobilized metal affinity chromatography followed by thrombin-catalyzed cleavage and size exclusion chromatography. The final buffer for protein samples contained 25 mM Na-HEPES, pH 7.0, 50 mM NaCl, and 0.5 mM tris(2-carboxyethyl)phosphine. Protein samples were either used in SAXS shortly after purification or stored at −80 °C in the presence of 5% glycerol until required.

For co-crystallization experiments with glucose and GKAs A, B, and C used in this report, the wild type human β-islet isoform of GK was cloned from residue 12 to the C terminus (22). The construct was codon-optimized for expression in *Escherichia coli* and cloned into a pET28B vector. The construct carries a sequence of MHHHHHHENLYFQGM from the expression vector to facilitate purification by metal affinity chromatography. Expression was obtained in *E. coli* BL21 DE3 cells with induction with 0.1 mM isopropyl β-D-thiogalactopyranoside at 18 °C overnight, and the expressed protein was purified with the N-terminal His tag intact.

Crystallization and Structure Determination—Crystals of GK in complex with glucose and GKAs A, B, and C were obtained by co-crystallization, which results in a crystal form of an orthorhombic space group (Table 1). In this crystal form, GK adopts the same active closed conformation as observed in most other glucose-bound GK structures (22). Prior to crystallization, GK protein was exchanged into 25 mM HEPES, pH 7.0, 0.5 mM tris(2-carboxyethyl)phosphine, 0.05 M NaCl, and 40 mM glucose; then concentrated to 20 mg/ml; and incubated with 1 mM GKA. Crystallization drops in a 1:1 ratio were set up over wells containing 0.1 M Tris HCl, pH 7.0, 80–200 mM glucose, and 19–26% PEG 4000. Crystals were cryoprotected by briefly soaking the crystals in well solution supplemented with 12.5% ethylene glycol and flash cooled by plunging into liquid nitrogen. In our hands, this orthorhombic crystal form is much more versatile in getting different GKA complex crystals and generally diffracts to higher resolution than the reported hexagonal crystal form (13–15).

To obtain GK-GKA-glucose-ATPγS complex crystals, preformed GK-GKA-glucose crystals of the reported hexagonal space group (13–15) were soaked in 1 mM ATPγS-Mg^{2+} in cryoprotectant solution overnight before being flash cooled in liquid nitrogen (Table 1). GK in this crystal form adopts the active closed conformation, very similar to that observed in the orthorhombic form. This hexagonal crystal form was obtained by the hanging drop vapor diffusion method by mixing 10 mg/ml GK in 25 mM HEPES, pH 7.0, 0.5 mM tris(2-carboxyethyl)phosphine, 0.05 M NaCl, 40 mM glucose, and 1 mM GKA at a 1:1 ratio with a well solution of 0.2 M ammonium acetate, 0.1 M Bis-Tris, pH 6.5, and 19–26% PEG 4000. Nucleotides were found to achieve full occupancy using this method.

Crystallization of GK-GKA-glucose in the active wide open conformation was carried out under conditions similar to those reported in Ref. 16. The crystallization wells contained 24% PEG 3350, 0.025 M citrate, pH 5.4, 0.2 M ammonium iodide, and 50 mM glucose, and crystallization drops were formed by mixing protein solution with an equal amount of well solution.

Crystallographic data sets were collected either in house on a Saturn 944 CCD detector using an FR-E rotating anode (compound B) (Rigaku, Austin, TX) or at a synchrotron beamline (Advanced Photon Source Industrial Macromolecular Crystallography Association 17ID (Chicago, IL), National Synchrotron Light Source 25X (Brookhaven, NY), or Advanced Light Source 5.0.1 (Berkeley, CA)), and processed with HKL2000 (41) or autoPROC (42). Ligands were built into electron density calcu-

TABLE 1
X-ray data collection and refinement statistics
r.m.s.d, root mean square deviation.

	Crystal[a]				
	A complex	B complex	C complex	Catalytic complex	Active wide open
Protein Data Bank code	3VEV	4DHY	3VF6	3VEY	4DCH
Crystal parameters					
Space group	$P2_12_12_1$	$P2_12_12_1$	$P2_12_12_1$	$P6_522$	$P2_1$
a, *b*, *c* (Å)	67.0, 82.1, 86.1	67.0, 82.1, 86.1	67.0, 82.1, 86.1	88.4, 88.4, 324.3	49.9, 85.8, 72.9
α, β, γ (°)	90, 90, 90	90, 90, 90	90, 90, 90	90, 90, 120	90, 104.4, 90
Overall B factor(Å^2)	22.1	32.4	21.0	68.1	29.6
Data collection statistics					
Resolution (Å)[b]	1.76 (1.86–1.76)	2.38 (2.51–2.38)	1.86 (1.96–1.86)	2.3 (2.42–2.3)	1.80 (1.84–1.80)
R_{merge} (%)[c]	5.6 (43.6)	10.9 (40.3)	7.1 (52.2)	8.2 (44.3)	6.8 (40.8)
I/σ	22.1 (2.1)	12.5 (3.1)	18.5 (2.5)	24.0 (2.0)	16.9 (1.4)
Completeness (%)	99.3 (89.8)	96.8 (92.5)	96.1 (76.4)	92.1 (81.0)	97.2 (75.5)
Redundancy	6.7 (2.6)	5.3 (3.8)	6.8 (4.2)	8.2 (3.0)	3.4 (2.2)
Refinement statistics					
No. reflections used ($F > 0$)	44,808	22,127	41,536	28,356	51,505
R_{work} (%)[d]	17.3 (18.3)	18.3 (19.8)	19.2 (24.8)	21.6 (25.4)	19.8 (27.0)
R_{free} (%)[e]	20.0 (22.2)	24.4 (24.1)	22.8 (27.1)	24.6 (24.4)	23.2 (35.4)
Residues	455	455	455	447	461
Waters	362	182	235	87	311
Ligands	Glucose and GKA	Glucose and GKA	Glucose and GKA	Glucose, GKA, and ATPγS	Glucose, GKA, and I^-
Mean B value (Å^2)[f]	27, 25, 37	29, 27, 31	26, 20, 31	68, 62,59	29, 25, 36
r.m.s.d. bond (Å), angle (°)	0.01, 1.05	0.01, 1.18	0.01, 1.01	0.008, 1.05	0.015, 1.47
Ramachandran plot (%)[g]	98.9, 0.2	97.3, 0.9	97.4, 0.4	97.1, 0.4	98.8, 0.5

[a] GK in complexes A, B, and C and catalytic complex adopts the active closed conformation. In all these crystals, there is only one complex per asymmetric unit.
[b] Statistics in the highest resolution bins are shown in parentheses.
[c] $R_{merge} = \sum_{hkl}\sum_i|I_i(hkl) - I(hkl)|/\sum_{hkl}\sum_i I_i(hkl)$ where $I_i(hkl)$ is the *i*th intensity measurement of reflection (*hkl*), and $I(hkl)$ is the mean intensity from multiple observations of that reflection.
[d] $R_{work} = \sum_{hkl}||F_{obs}| - |F_{calc}||/\sum_{hkl}\sum|F_{obs}|$ where F_{obs} and F_{calc} are observed and calculated structure factor amplitudes, respectively.
[e] R_{free} is calculated using 5% of reflections randomly excluded from refinement. For crystals with the same space group and similar unit cells, the same set of reflections was chosen for exclusion.
[f] Average temperature factors for protein atoms, ligands, and waters, respectively.
[g] Percentages of residues in the most favorable and disallowed regions of the Ramachandran plot, respectively.

lated from a protein model with ligands and water molecules removed using Coot (43) and refined with BUSTER (44) or REFMAC (45) with TLS restraints. Data collection and refinements statistics are listed in Table 1.

Compounds A, B, C, and D—Compounds A, B, C, and D, all of which are glucokinase activators, were developed and synthesized as reported (17–20). Purities of these compounds were confirmed by mass spectrometry and NMR.

SAXS Data Collection—Initial SAXS experiments were performed at beamline X21 at Brookhaven National Laboratory. Protein concentrations were evaluated at 0.5–10 mg/ml using a flow cell format with exposure times of 30–120 s. Within this concentration range and exposure time, no aggregation, interparticle interference, or radiation damage was observed. Subsequent data were collected at beamline 12.3 at Advanced Light Source or X9 at the National Synchrotron Light Source. To minimize aggregation, protein samples were prepared less than 2 days ahead of planned experiments and were spun in a tabletop microcentrifuge for 5 min at maximum speed immediately before data collection. The scattering data were collected on a Marccd detector, and the scattering angle was calibrated using a silver behenate sample. At National Synchrotron Light Source X9, a second detector was set up at closer distance to collect the wide angle part of the scattering (46). For buffer scattering subtractions (36–38), identical buffer samples were prepared, and their scattering was measured immediately before or after measurements of the corresponding protein samples. For each sample, measurements were repeated two to three times for accuracy. The scattering data were circularly averaged over the detector and normalized by the transmitted incident beam intensity using programs developed at the beamlines.

SAXS Data Analysis—All data analysis was carried out using the SAXS program package Atsas developed at the European Molecular Biology Laboratory by Svergun and co-worker (38). The net protein scattering data, $I(q)$, were generated by subtraction from scattering of the same buffer using PRIMUS (38) or software developed at beamline X9 at the National Synchrotron Light Source (46).

Modeling of SAXS Data—Fitting of experimental SAXS curves to theoretical curves calculated from crystal structures was carried out using CRYSOL (39). To determine the solution conformation of GK at saturating glucose, the active closed and active wide open conformation were used to generate the morphs of conformations in between these conformations using LSQMAN (47). To determine glucose binding affinity, non-linear regression curve fittings were carried out using GraphPad Prism (GraphPad Software, San Diego, CA).

RESULTS

Catalytic Complex of GK Adopts Active Closed Conformation—In our efforts to develop GKAs to treat diabetes, many GKA-glucose-GK complex crystal structures have been generated, including those with compounds used in our SAXS studies discussed below (18–20). GK adopts the reported active closed conformation in most of these structures (Table 1). In this conformation, glucose is completely buried and interacts with key residues from both the small and large domains of GK (Fig. 1*A*). To fully understand the catalytic mechanism and the relevance

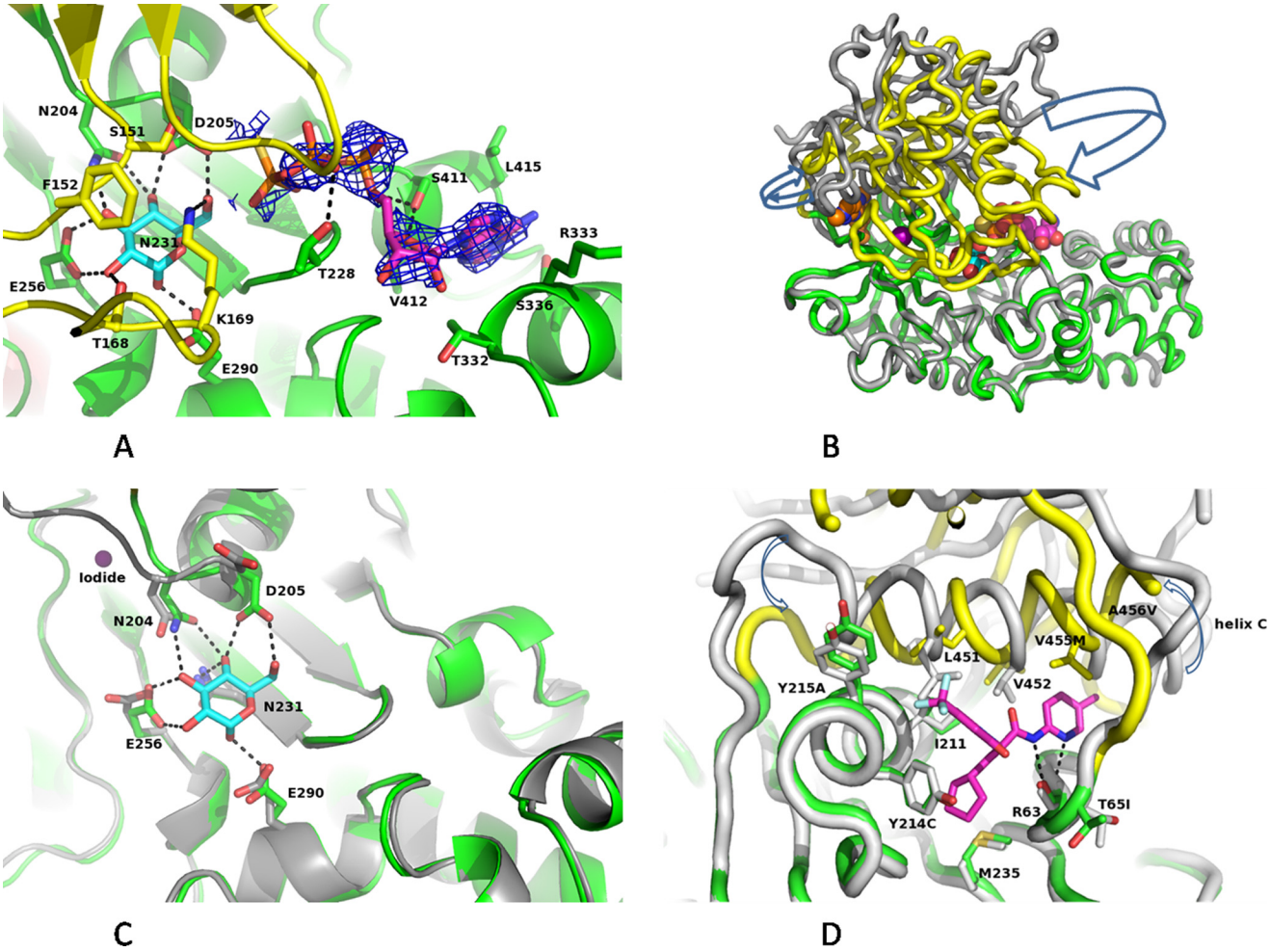

FIGURE 1. **Different conformations observed in GK crystals.** *A*, the active site of GK in the active closed conformation that represents the catalytic complex. The nucleotide binding site ($2F_o - F_c$ omit map contoured at 1.2σ) was illuminated by soaking in 1 mM ATPγS-Mg^{2+} (carbon atoms are colored in *magenta*, oxygen is in *red*, and nitrogen is in *blue*) in preformed glucose-bound GK crystals (carbon atoms of glucose are in *cyan*). The secondary structures of GK are shown with the small domain colored *yellow* and the large domain in *green*. Key residues that interact with substrates are also shown, and hydrogen bonds are shown in *dashed lines*. Pictures in this figure were prepared using PyMOL (51). *B*, overlay of the overall structures of the active closed conformation and the active wide open conformation (*gray ribbons*). An iodide ion (colored in *purple*) was found at the interface of the small and large domains only in the active wide open conformation. GKA, iodide, glucose, and ATPγS are shown in *space-filling models* from *left* to *right*. Rotation of the small domain from the active wide open to the active closed conformation is highlighted with *arrows*. *C*, overlay of the active site of GK in the active wide open conformation with that in the apo conformation (*gray ribbons* and carbon atoms). Active site residues from the small domain are far away from the active site in both conformations. In addition, in the apo conformation, Asp^{205} in the large domain does not interact with glucose; instead, it forms a unique salt bridge interaction with Arg^{477} of helix C (not shown). *D*, an example of a GKA (compound A) bound at the allosteric site of GK in the active closed conformation. The allosteric site in the active wide open conformation is overlaid (*gray*) to show the changes at the allosteric site brought by overall conformational changes. Side chains of key residues that interact with the GKA are highlighted. Naturally occurring activating mutations of GK, such as T65I and Y214C, are labeled.

of the active closed conformation in the reaction cycle, we performed structural analysis of a glucose-GKA-ATP-GK complex formed by soaking an ATP analog, ATPγS, into preformed GK-glucose-GKA crystals. ATPγS bound at a site adjacent to the glucose site with the base and ribose recognized by residues exclusively from the large domain (Fig. 1*A*). Importantly, there was no hydrogen bond interaction between the adenine base and GK, explaining the less stringent specificity of GK (and other hexokinases) toward nucleotide substrates (33–35). The α,β-phosphate and γ-thiophosphoryl groups of ATPγS interacted with residues from both the small and large domains. The γ-thiophosphate of ATPγS had relatively weaker electron density (Fig. 1*A*) probably due to partial hydrolysis. Nevertheless, it was located close to the 6′-hydroxyl of glucose, anchored by hydrogen bonds from the peptide backbone at Thr^{228} and Gly^{229}, and ready for the nucleophilic reaction. This observation indicated that the active conformation represents the catalytic complex of GK.

To better define interactions between the γ-phosphate and the 6′-hydroxyl of glucose, we repeatedly tried to co-crystallize or soak with AMPPNP, another non-hydrolyzable ATP analog, to gain improved definition of the transferable phospho group. Unfortunately, these efforts failed to generate strong electron density for AMPPNP in two different crystal forms of the active closed conformation. Similar attempts from other laboratories resulted in the same weak electron density for AMPPNP (22). In solution, AMPPNP was reported to have a binding affinity of 0.27 mM, which is similar to the 0.78 mM binding affinity of ATP (32). It is possible that AMPPNP is simply incompatible with the compact active site of the active closed conformation, which is probably stabilized by the crystal contacts.

Observation of Active Wide Open Conformation in Crystals—Interestingly, a wide open conformation was also observed in crystals of several glucose-GKA-GK complexes. In these crystals, the small domain rotates 44° as a rigid body away from the active site of GK (Fig. 1*B*). As a result, all the active site residues in the small domain are far away from glucose (Fig. 1*C*). On the other hand, all the active site residues in the large domain remain in interaction with glucose (Fig. 1*C*). This contrasts with the apo conformation in which two active site residues in the large domain, Asp^{205} and Glu^{256}, do not interact with glucose (Fig. 1*C*). Also unlike the apo conformation, there is no large scale rearrangement of secondary structure elements in the small domain, and both the large and small domains can be superimposed separately between this wide open conformation and the active closed conformation (root mean square deviation, 0.83 and 1.3 Å for 294 and 100 Cα atoms of the large and small domains, respectively). A reversed 44° rigid body rotation can bring all the active site residues in the small domain back to the active site (Fig. 1*A*). This rigid body rotation requires local movements of two flexible loops that connect the small and large domains (Fig. 1*D*). Because only a rigid body motion is needed in the conversion of this wide open conformation to the active closed conformation and this conformation is expected to have higher glucose affinity than the apo conformation, we name it the active wide open conformation. It is expected that conversion between the active closed and the active wide open conformation would be much faster than that between the apo and the active closed conformation. The active wide open conformation would represent a species in the catalytic reaction except for the fact that the crystallization of this conformation requires a high concentration of iodide, and an iodide ion was found at an interface that exists only in the active closed conformation between the small and large domains (Fig. 1, *B* and *C*). At a minimum, the degree of rotation of the small domain would be influenced by the presence of the iodide, and this conformation may not be the dominant one in its absence.

Allosteric GKA Site—In both the active closed and active wide open conformations, all known GKAs bind at the same allosteric site formed by residues from the small and large domains and two loops that connect them (Fig. 1*D*). This allosteric site exists only in GK (13–22) and not in other hexokinases (33–35). In the apo conformation, residues in the small domain are not positioned to form the allosteric site, especially helix C (14). GKA binding stabilizes this allosteric site and in turn stabilizes those active conformations. Most activating mutations of GK also occur at this allosteric site (Fig. 1*D*). Because the two connecting loops (peptides 66–71 and 438–441) that make the local movements to accomplish the rigid body rotation of the small domain reside at the allosteric site, the allosteric site is much closer to the rotation axis. As a result, conversion from the active wide open conformation to the active closed conformation only slightly enlarges the allosteric site while moving the active site residues from the small domain over much longer distances to close the active site (Fig. 1*D* and supplemental movie). This explains why small changes in GKAs have large effects on their ability to activate GK and also explains why small changes caused by naturally occurring activating mutations at the allosteric site can result in large changes in the kinetics of GK (Fig. 1*D*) if we accept that the chemical reaction is not the rate-determining step of the overall catalytic process.

GK Is Monomeric in Solution—To investigate the effects of glucose, nucleotides, and small molecule agonists on the solution conformation of GK, SAXS data sets were collected on fresh GK samples in the presence of glucose at difference concentrations. The small angle scattering intensity, $I(q)$, was measured for scattering angles ($q = 4\pi\sin\theta/\lambda$) from 0.01 to 0.3 A^{-1} on a Marccd detector (Fig. 2*A*). For some data sets, wide angle scattering (q up to 1.5 $Å^{-1}$) was also recorded on a CCD detector positioned close to the protein sample, but most of the wide angle scattering signals were too weak and noisy to be useful (Fig. 2*A*). In the following analysis, the upper resolution limit was set at $q = 0.5–0.6$ $Å^{-1}$. As an initial inspection, Guinier plots were generated on all scattering curves to detect potential protein aggregates (Fig. 2*B*). Good linearity of the Guinier plots and protein sizes calculated based on these plots indicated that freshly purified GK samples were monodispersive with no aggregation within the concentration range tested (0.5–10 mg/ml) and had no significant interparticle interference up to 10 mg/ml (36–38). Within the exposure times used (1–3 min for stationary sample chamber or 5–20 μl/min flow rate for flow cells), repeated measurements of the same protein sample did not show time-dependent changes of the size and overall shape of the protein, indicating that there was no radiation damage (36–38). GK was apparently a well folded protein under the conditions used, and glucose dose-dependently induced GK to become more compact (Fig. 2*C*). By all these criteria, fresh GK samples appeared to be a well behaved monomeric and monodispersive protein under the conditions used. Aggregation was detected in samples kept for more than a week at 4 °C, but GK samples remained monodispersive for more than a year if they were kept frozen at −80 °C. Based on these initial assessments, all the following GK SAXS data were routinely measured at around 5 mg/ml protein with 180-s exposure time and at a 10 μl/min flow rate in a flow cell.

GK Has Two Discrete Sizes in Solution—GK clearly became more compact when the glucose concentration increased as reflected by the decreasing slopes of the linear Guinier plots, the increase in peak heights in Krakty plots, and the $P(r)$ function as well as the decrease of D_{max} with increasing glucose concentration (Fig. 2, *B*, *C*, and *D*). The overall sizes of GK at different glucose concentrations, measured as the radius of gyration (R_g) of the protein, which can be calculated from the Guinier plots, decreased with increasing concentration of glucose (Fig. 2*B*). The R_g-glucose concentration-response curve was fit nicely using a one-site binding model by the non-linear regression algorithm implemented in GraphPad Prism (GraphPad Software) (Fig. 2, *C* and *D*). The K_d for glucose thus derived, 5.2 ± 0.4 mM, was slightly smaller than the $K_{0.5}$ of GK for glucose determined in biochemical assays (1, 2) and very close to that derived from a fluorescence quenching study on GK (4.5 mM; Refs. 29 and 31). The difference between R_g values of wild type GK determined at 0 mM glucose and at a saturating level of glucose was 1.53 ± 0.03 Å, which was significantly larger than the standard error associated with R_g measurements in our experiments (~0.2–0.4 Å). These results indicated that GK in solution existed as a mixture of two populations of particles

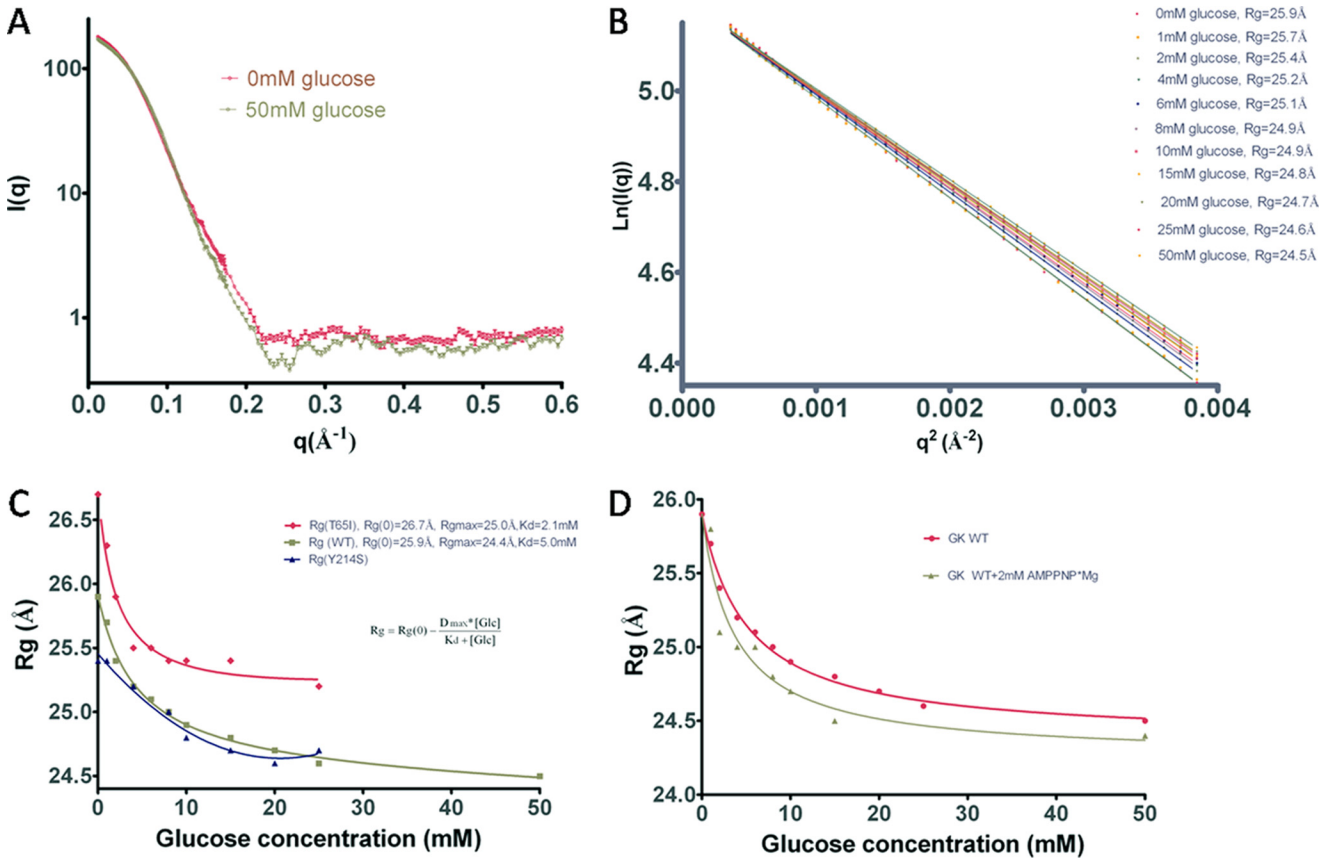

FIGURE 2. **Effect of glucose concentration on SAXS of GK.** *A*, typical scattering curves for GK (5 mg/ml) after subtraction of buffer scattering. *B*, Guinier plots of wild type GK scattering at different glucose concentrations. The r^2 values (the goodness of linear regression fitting) are >0.999 for all curves, and the R_g values derived from the slopes of the linear fitting all have standard errors of less than 0.2 Å. *C*, the R_g-glucose concentration response of wild type GK (WT) and T65I and Y214S mutants is fitted using a non-linear regression algorithm with a one specific binding site model. The R_g-glucose responses indicate that GK has one specific glucose binding site, and glucose dose-dependently shifts GK from the apo conformation with a larger R_g to that of a glucose-bound conformation with a smaller R_g. The binding affinity of glucose to GK can be determined. *D*, nucleotides do not shift the conformational equilibrium of GK. The non-hydrolyzable ATP analog AMPPNP-Mg^{2+} (2 mM) was used in these experiments to avoid glucose turnover.

with distinct sizes; one was the more compact, glucose-bound GK, and the other was apoGK. The R_g of apoGK is 25.9 Å, and that of glucose-bound wild type GK is reduced to 24.4 Å (Fig. 2*C*). The existence of these two distinct sizes of GK molecules in solution implies two different conformations, an apo and a glucose-bound conformation.

ApoGK in Solution Adopts Apo Conformation Observed in Crystal—ApoGK in solution clearly adopted a conformation distinctly less compact than that of glucose-bound GK, consistent with the distinct apo conformation found in the apoGK crystal structure. In addition to R_g, which can be derived from the low resolution portion of the scattering curves, additional structure information can be derived from the entire scattering curve. To confirm that GK adopts the apo conformation seen in the crystal structure, the theoretical scattering from the crystal structure of apoGK (Protein Data Bank code 1V4T) was fitted to the entire experimental SAXS curve of glucose-free GK using CRYSOL (39) within a resolution range of 0–0.5 $Å^{-1}$. Due to disorder, a 23-amino acid region in the middle of GK (Glu^{157}–Asn^{179}) was not located in the apoGK crystal structure (14), but these amino acids should also contribute to x-ray scattering in solution (34–36). The missing region was therefore reconstructed from the active closed conformation. The fitting of the experimental scattering improved significantly with this reconstructed model (goodness of fit, $\chi^2 = 2.2$; Fig. 3*A*). As a comparison, fitting of the active wide open and the active closed structure resulted in χ^2 values of 7 and 18, respectively. The calculations indicated that GK in the absence of glucose adopted almost entirely the inactive, super-open conformation.

Glucose-bound GK Adopts Active Open Conformation—Glucose-bound GK is much more compact than apoGK. Surprisingly, neither the active wide conformation model nor the active closed conformation model fit well with the glucose-bound GK SAXS data ($\chi^2 = 5.2$ and 6.6 for the active closed and wide open forms, respectively; Fig. 3*B*), and the reconstructed apo model fit even less well ($\chi^2 = 12.7$; Fig. 3*B*). As the active closed conformation represents the most compact form of GK and it only takes a rigid body rotation to convert it to the active wide open conformation, we assumed that a predominant active open form exists between these two conformations. To find the conformation that fit the SAXS curve for glucose-bound GK, different glucose-bound GK models were generated by interpolating between the wide open and the active closed conformations using the morph algorithm implemented in LSQMAN (47). The best fitting solution was then identified by fitting the theoretical scattering curves from each of these conformations to the experimental curve. The best solution was a conformation with an opening angle of ~17° relative to the

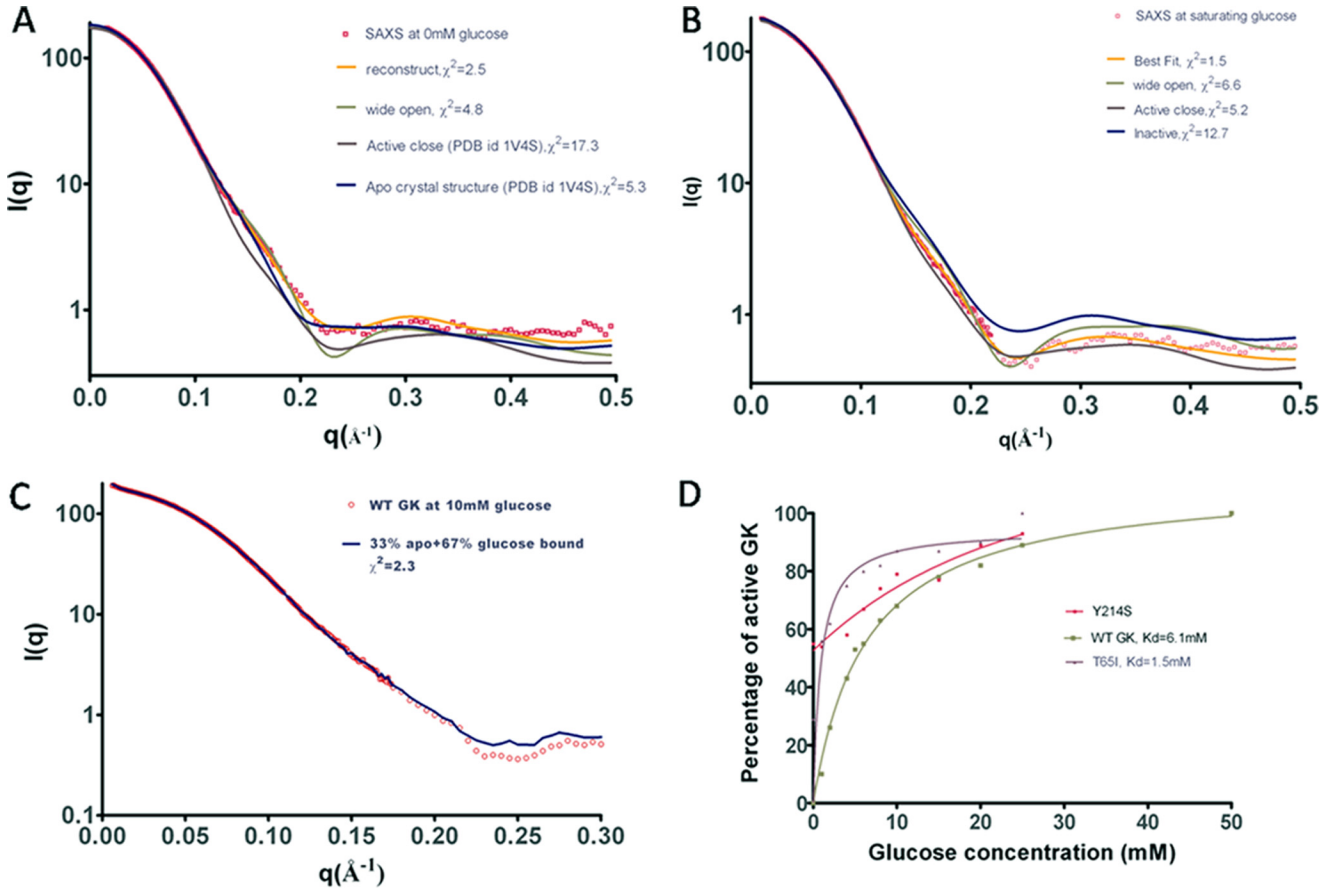

FIGURE 3. **SAXS models of apo and active open conformations of GK in solution.** *A*, fitting crystal structures of GK to the apoGK SAXS curve. Theoretical scattering curves were generated from the apoGK crystal structure (an incomplete model in which 23 residues were disordered), from a model with the missing residues reconstructed (reconstructed model), from the active wide open structure, or from the active closed model. The errors of fit, χ^2, are listed. *B*, fitting of scattering curves for glucose-bound GK (glucose concentration, 100 mM). Best fitting was obtained with an active open conformation derived from morphing between the active closed and the active wide open conformation. The active open conformation was opened by ~17° from the active closed conformation. *C*, example of fitting the GK conformation at an intermediate glucose concentration as a mixture of the apo and glucose-bound GK conformations. *D*, percentages of glucose-bound GK conformation (active open) as a function of glucose concentration for wild type, T65I, and Y214S GK.

active closed conformation, and this had an excellent fit to the experimental curve (χ^2 = 1.5; Fig. 3*B*). In comparison, the opening is ~12° in hexokinases (34, 35). A similar approach was used in studies of the conformational dynamics of Hsp90 in solution (40). This result indicated that in solution glucose-bound GK adopts a predominantly active open conformation or an ensemble of conformations closely related to it. This conformation is probably required for the catalytic reaction, facilitating the departure of products from and entry of substrates to the active site. Transition of the GK conformation from the active open to the active closed conformation results in completion of the glucose and phosphate binding sites. GK is expected to have higher affinity toward glucose at the active closed conformation than at the active open conformation. In the meantime, the allosteric site for GKAs is enlarged during this conversion (Fig. 1*D* and see the supplemental movie for the GK conformation conversion pathway).

Glucose Dose-dependently Shifts Conformational Equilibrium of GK—To extend support for the interpretation that GK in solution has two conformational populations or two ensembles of conformations, we fit the SAXS curves at intermediate glucose concentrations as a linear combination of the apo and the active open conformations using OLIGOMER in the European Molecular Biology Laboratory SAXS program suite Atsas22 (38). Satisfactory fits were obtained (Fig. 3*C*) and gave the percentages of each conformation at particular glucose concentrations. Furthermore, the response of the percentage of active GK conformation to variation in the glucose concentration fit well to a model based on one specific glucose binding mode using a non-linear regression algorithm with an apparent K_d of 6.0 mM for glucose (Fig. 3*D*). With this model, GK adopted 100% apo conformation at 0 mM glucose and approached 100% conversion to the active open conformation when the glucose concentration approached saturating levels. This result indicated that GK populates two discrete major conformations in solution rather than exploring a continuum of intermediate conformations, a conclusion that is consistent with the model of a single glucose binding site.

AMPPNP Does Not Change Conformational Distribution of GK—We measured the scattering of glucose-free GK in the presence of 2 mM ATP-Mg^{2+} or GK in the presence of 2 mM AMPPNP-Mg^{2+} at different glucose concentrations. Consistent with the biochemical findings that ATP is a classical substrate of GK, neither ATP nor AMPPNP induced a global conformational change in GK in the absence of glucose, and AMPPNP did not change the distribution of GK conformations

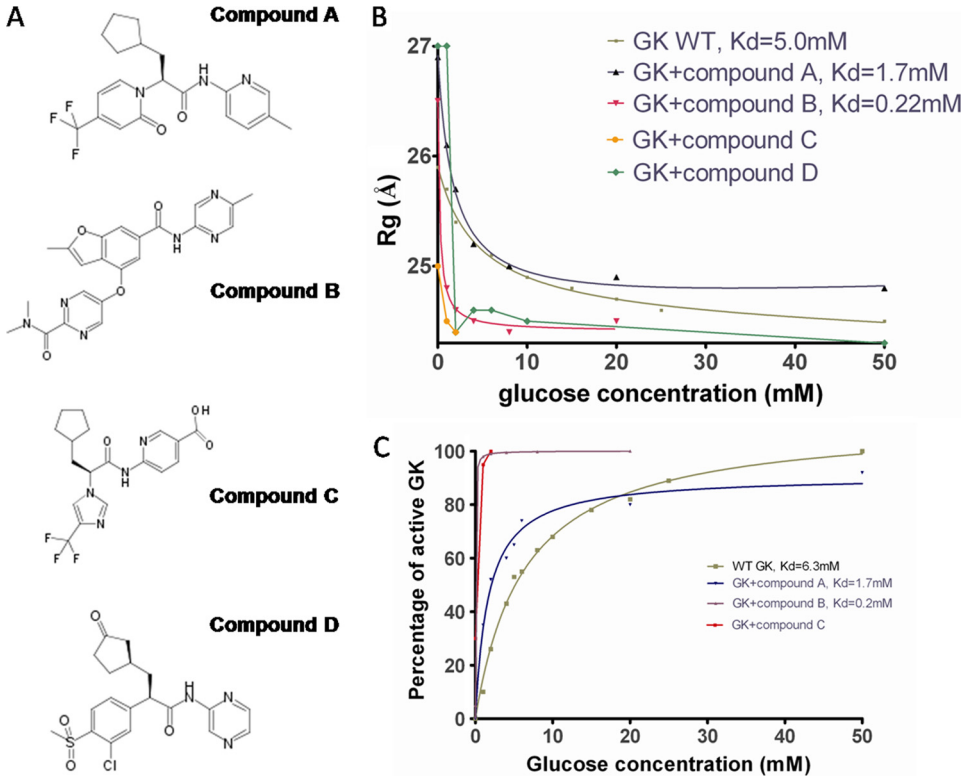

FIGURE 4. **Small molecule GKAs shift equilibrium for GK activation to lower glucose concentrations.** *A*, chemical structures of GKAs studied in this report. Compound A, $\alpha = 0.26$, $\beta = 1.2$, $EC_{50} = 691$ nM (18); compound B, $\alpha = 0.1$, $\beta = 0.87$, $EC_{50} = 174$ nM (19); compound C, $\alpha = 0.03$, $\beta = 1.56$, $EC_{50} = 92$ nM (20); and compound D, $\alpha = 0.036$, $\beta = 1.71$, $EC_{50} = 343$ nM (17). *B*, R_g-glucose response of GK in the presence of 400 μM GKA. Compound C induces the active conformation at 0 mM glucose and cannot fit with a glucose binding site model. Compound D aggregates GK at 0 and 1 mM glucose, but aggregation is apparently rescued by glucose at 2 mM glucose or above. *C*, percentage of active GK conformation plotted as a function of glucose concentration in the presence of compounds A, B, and C.

at different glucose concentrations either (Fig. 2*D*). Using the modeling method described above, the GK-AMPPNP-glucose ternary complex was found to be slightly more compact than the GK-glucose binary complex but still not as compact as the active closed conformation. Caution is warranted in interpreting the effect of AMPPNP on the conformation of GK in the presence of glucose because crystallographic observations indicate that AMPPNP is not an ideal ATP analog in terms of inducing the active closed conformation (32).

Activating Mutations Shift GK to Active Conformation at Lower Glucose Concentrations—Activating mutants of GK can cause hypoglycemia (11, 12) but with varying degrees of severity. The activating mutants T65I and Y214C exemplify two extremes in the spectrum of this effect. T65I caused only mild, manageable hypoglycemia (11), whereas T214C caused severe hyperinsulinemic hypoglycemia that was unresponsive to treatments (12). Thr^{65} is located on a loop connecting the small and large domains of GK at the allosteric site (Fig. 1*D*). Tyr^{214} is located centrally at the allosteric binding site and interacts directly with all GKAs discovered to date (Fig. 1*D*) (13–22). We produced the T65I and the Y214S GK mutants (Y214C is prone to protein aggregation) and measured their SAXS profiles. In biochemical comparisons with wild type GK, T65I and Y214C exhibited lower $S_{0.5}$ values (3.8 and 2.1 mM, respectively, *versus* 7.1 mM for wild type) as well as suppressed cooperativity (0.9 and 1.2, respectively, *versus* 1.7). Their V_{max} values also decreased, especially T65I (5.9 and 28 s^{-1}, respectively, *versus* 33 s^{-1}) (26). In our SAXS experiments, both T65I and Y214S mutants became more compact with increasing glucose concentrations. However, although the apo T65I protein adopted a conformation similar to that of the wild type apoGK (R_g of 26.2 *versus* 25.9), apo Y214S seemed to be more compact than the wild type. The R_g-glucose response curve for T65I could be fit with a single site binding model, but the glucose response of Y214S R_g could not be fit to the same model (Figs. 2*C* and 3D). It appeared likely that some of the Y214S molecules adopted the active open conformation in the absence of glucose.

GKAs Shift GK to Active Conformation at Lower Glucose Concentrations—Full agonist GK activators lower glucose and enhance GSIS but create a risk of hypoglycemia by severely depressing the $S_{0.5}$ of GK (13–17). To avoid this risk and increase the therapeutic window of GKAs, current efforts focus either on partial agonists that suppress $S_{0.5}$ relatively mildly or on hepatoselective GKAs. Compounds A, B, C, and D (Fig. 4*A*) have very different enzymatic effects and tissue selectivities (17–20) and were chosen for GK SAXS studies to investigate correlations between conformational states of GK and the effects of these compounds on GK activation. The abilities of compounds to reduce K_m ($S_{0.5}$) and elevate V_{max} are represented by their α and β values as defined by the non-essential activator model of Segal (48) and experimentally determined in biochemical assays (20, 21). Compound A, an example of a partial GK agonist, was discovered through lead optimization after a high throughput screening (18). It has an α value of 0.26 and a

β value of 1.23, indicating a mild depression of $S_{0.5}$ combined with effective activation of GK at high glucose concentrations but with weak activation of GK at lower glucose concentrations. Compound B ($\alpha = 0.1$ and $\beta = 0.87$) depresses K_m more than compound A but less than compounds C and D (17, 19, 20) and has entered clinical trials for the treatment of diabetes (19). With small α values (0.03 and 0.04, respectively) and large β values (1.56 and 1.71, respectively), compounds C and D are typical full GK agonists. Both compounds significantly reduce K_m and increase V_{max} for GK (17, 20). However, compound C was designed to be hepatoselective: the addition of a carboxylate group renders it unable to enter β-islet cells, but it can enter liver cells through active transport (20). Compound C is expected to fully activate GK in liver but without the complication of overly stimulating GSIS (20). Compound D, a typical systematic full GK agonist developed by Hoffmann-La Roche, was shown to fully activate both glucose uptake in liver and insulin secretion in β-islets (17). In SAXS experiments, consistent with their ability to activate GK, all four GKAs shifted the conformational equilibrium of GK to the active open conformation at lower glucose concentrations (Fig. 4). However, their SAXS profiles differed in consistence with their distinct biochemical profiles. Significantly, in the presence of compound A, the apparent K_d of glucose for GK determined by SAXS is 1.7 mM, consistent with its α value of 0.26 as determined by biochemical assay. Compound B shifts the activation equilibrium much more than compound A as reflected in the lowered K_d of glucose for GK. Compound C in agreement with its low EC_{50} and especially low α value converts a substantial amount of GK even at 0 mM glucose, indicating its ability to bind to GK without glucose. It is noteworthy that compound D actually aggregated GK at low glucose concentrations (0–1 mM) at the compound concentrations used in SAXS (~400 μM), but the protein became monomeric at 2 mM glucose or above, indicating a protective role of the formation of the GK-GKA-glucose ternary complex against aggregation (Fig. 4).

Careful inspections of the SAXS profiles of GK in the presence of different GKAs indicated small conformational differences between the respective GK-GKA-glucose complexes of different GKAs (Fig. 4). These were correlated with the α values of the GKAs. For example, compound A (which has a significantly higher α value than compounds B, C, and D) gave a GK-glucose-compound A complex that is significantly less compact than those of compounds B, C, and D (Fig. 4). These conformational differences detected by SAXS have been consistently observed with other compounds tested.

Modified Mnemonic Model for Cooperativity in GK—Based on the conformations observed in both crystals and solution and structural analysis of the binding sites for glucose, ATP, and GKAs, we propose a modified mnemonic model to describe cooperativity in GK (Fig. 5). In this model, E′, E, and E* are the apo, the active open, and the active closed conformations, respectively. This model differs from the ligand-induced slow transition model in that there is only one reaction cycle, and it involves the E and E* species (31). It also differs from the old mnemonic model in that glucose can bind to E′ albeit with lower affinity. Structural analyses indicate that the formation of a catalytically competent species both triggers and requires the conversion of E′ to E or E*. Among the active site residues, Asp^{205} is a key residue that is involved in both the catalytic reaction (Fig. 1*A* and Ref. 33), and in the stabilization of E′ in the absence of glucose (Fig. 1*C* and Ref. 14). Flipping the Asp^{205} side chain from interacting with Arg^{477} in helix C in E′ to the active site would destabilize E′ and trigger the conversion from E′ to E or E* (Fig. 1*C* and Ref. 14). In E′, helix C is at a position that blocks the small domain from closing down to the large domain to form E* (14). Structural analysis of the allosteric site indicated that GKAs can only bind to the E and E* species of GK (Fig. 1*D*), but our SAXS experiments also indicated that some GKAs, especially some full GK agonists, can bind and stabilize E or E* in the absence of glucose (Fig. 3). Both GKAs and GK-activating mutations shift the equilibrium from E′ toward E by stabilizing E. As our current SAXS studies concentrated on GK at equilibrium, they were not able to detect some kinetic intermediate conformations or some minor species due to signal sensitivity (27–32).

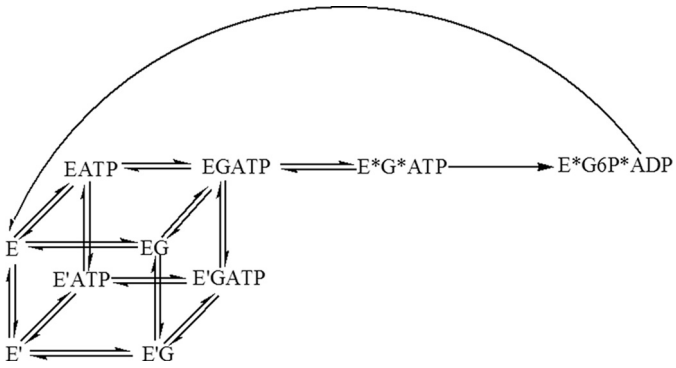

FIGURE 5. **Modified mnemonic kinetic model for cooperativity of GK.** E′, E, and E* stand for the apo, the active open, and the active closed conformations of GK, respectively. In this model, there is only one catalytic cycle involving the E and E* species. E′ has to be converted to E to enter the reaction cycle. Product ADP can bind to E′, E, and E* in the presence or absence of glucose, and GKAs can only bind to E and E* in the presence or absence of glucose or nucleotides. For simplicity, equilibria involving ADP and GKA are omitted. *G*, glucose; *G6P*, glucose 6-phosphate.

DISCUSSION

The crystal structure of the catalytic complex of GK reported here illustrates how the chemical reaction is catalyzed by GK. A similar active closed conformation has also been observed in other hexokinases, such as human brain hexokinase and yeast hexokinase (33–35). Using SAXS in combination with x-ray crystallography, we identified and modeled an active open conformation of GK in solution. A similar but not identical active open conformation has also been observed in crystal structures of human brain hexokinase I (35) and yeast hexokinase (34). These results suggest a reaction cycle that is conserved between GK and other hexokinases: the enzymes alternate between the active open and the active closed conformations to bind substrates and release products during the reaction cycle (Fig. 5, *top layer*). GK is unique in that outside this reaction cycle there is an apo conformation with low glucose affinity that converts slowly to the active open conformation (Fig. 5, *bottom layer*). Other hexokinases, such as human hexokinase I and yeast hexokinases, are known to be classical enzymes without cooperativity, and they lack the apo conformation. As a related

point, GK is the only hexokinase that has an allosteric activation site (Fig. 1*D*).

The apo conformation and the active open conformation of GK are also relevant to the regulation of GK in liver: the apo conformation can be recognized by GKRP, but apparently the active open conformation cannot (6). Consistent with this interpretation, GKAs promote the dissociation of GK from GKRP at lower glucose concentrations (49).

Our results demonstrate that SAXS complements crystallography by providing information free of concerns about crystallization and crystal contact artifacts, an aspect that is especially relevant for flexible proteins, such as GK. For example, we have concluded that the active wide open conformation observed in some complex crystals is most probably due to the iodide ion used in crystallization. SAXS showed that the active closed conformation was a minor species in solution, and its tendency to occur in most GK-glucose-GKA crystals is probably due to stabilization by crystal contacts that favor it as the most compact conformation. Moreover, no single active conformation suffices to explain the diversified kinetic profiles of different GKAs (17–22). SAXS measurements of GK in the presence of different GKAs have shown that GK adopts slightly different active conformations in solution. The ability of these compounds to induce different degrees of openness of GK in solution helps to explain their kinetic profiles and suggests ideas that may aid in the design of GKAs with different kinetic profiles. For example, modeling indicates that in conformations in which the allosteric site is larger the active site of GK is more closed, which should result in higher affinity for glucose (Fig. 1). Therefore, GKAs should induce higher glucose affinities (and lower α) in a manner proportional to their ability to enlarge the allosteric site of GK (for example, through interactions with helix C) and close the glucose site and vice versa (17–22). On the other hand, compounds that are predicted to interact with helix C very strongly should suppress β values (18) presumably by inhibiting the conformational conversions between the active open and active closed conformations and the overall reaction.

As also exemplified by the present studies, SAXS can directly detect global conformational changes induced by allosteric agonists, free from common biochemical assay artifacts, such as label interference and nonspecific binding. To identify GKA lead compounds, a high throughput biochemical assay has to be carried out at low glucose concentrations to maximize the window for hit detection. SAXS can operate at different glucose concentrations and would have a better chance of identifying "partial activator" compounds with high α values, such as compound A. With improvements in automation and other hardware and software support at synchrotron beamlines, we expect to see more use of SAXS as an alternative platform for assaying and screening GKAs and other allosteric agonists (50). Structural information for compounds A, B, and C was initially difficult to obtain by crystallography due to difficulty in co-crystallizing them with GK, but information about the conformational influences of these compounds was readily obtained in the SAXS experiments.

Acknowledgments—We thank Michael Hickey for help in the crystallization of the active wide open crystal form, Matt Griffor for help in construct design, and Angel Guzman-Perez and Meihua Tu for chemistry discussions. We greatly appreciate Lin Yang and Marc Allaire at the National Synchrotron Light Source X9 beamline and Michal Hammel, Greg Hura, and John Tainer at the Advanced Light Source Structurally Integrated Biology for Life Sciences beamline for help with SAXS data collection and processing. We also thank beamline scientists at the Advanced Photon Source Industrial Macromolecular Crystallography Association and National Synchrotron Light Source X25 for help with crystallographic data collection. Finally, we thank Kieran Geoghegan and Ann Aulabaugh for proofreading the manuscript and insightful discussions in enzyme kinetics.

REFERENCES

1. Matschinsky, F. M. (2005) Glucokinase, glucose homeostasis and diabetes mellitus. *Curr. Diab. Rep.* **5,** 171–176
2. Magnuson, M. A., and Matschinsky, F. M. (eds) (2004) in *Glucokinase and Glycemic Disease: From Basics to Novel Therapeutics* (*Frontiers in Diabetes*), Vol. 16, pp. 1–17, Karger, Basel, *Switzerland*
3. Jetton, T. L., Liang, Y., Pettepher, C. C., Zimmerman, E. C., Cox, F. G., Horvath, K., Matschinsky, F. M., and Magnuson, M. A. (1994) Analysis of upstream glucokinase promoter activity in transgenic mice and identification of glucokinase in rare neuroendocrine cells in the brain and gut. *J. Biol. Chem.* **269,** 3641–3654
4. Iynedjian, P. B., Gjinovci, A., and Renold, A. E. (1988) Stimulation by insulin of glucokinase gene transcription in liver of diabetic rats. *J. Biol. Chem.* **263,** 740–744
5. Henquin, J. C., Ravier, M. A., Nenquin, M., Jonas, J. C., and Gilon, P. (2003) Hierarchy of the beta-cell signals controlling insulin secretion. *Eur. J. Clin. Invest.* **33,** 742–750
6. Van Schaftingen, E., Detheux, M., and Veiga da Cunha, M. (1994) Short-term control of glucokinase activity: role of a regulatory protein. *FASEB J.* **8,** 414–419
7. Vionnet, N., Stoffel, M., Takeda, J., Yasuda, K., Bell, G. I., Zouali, H., Lesage, S., Velho, G., Iris, F., Passa, P., Froguel, P., and Cohen, D. (1992) Nonsense mutation in the glucokinase gene causes early-onset non-insulin-dependent diabetes mellitus. *Nature* **356,** 721–722
8. Froguel, P., Vaxillaire, M., Sun, F., Velho, G., Zouali, H., Butel M. O., Lesage S., Vionnet N., Clément, K., Fougerousse F., Tanizawa, Y., Weissenbach, J., Beckmann, J. S., Lathrop, G. M., Passa, P., Permutt, M. A., and Cohen, D. (1992) Close linkage of glucokinase locus on chromosome 7p to early-onset non-insulin-dependent diabetes mellitus. *Nature* **356,** 162–164
9. Hattersley, A. T., Turner, R. C., Permutt, M. A., Patel, P., Tanizawa, Y., Chiu, K. C., O'Rahilly, S., Watkins, P. J., and Wainscoat, J. S. (1992) Linkage of type 2 diabetes to the glucokinase gene. *Lancet* **339,** 1307–1310
10. Glaser, B., Kesavan, P., Heyman, M., Davis, E., Cuesta, A., Buchs, A., Stanley, C. A., Thornton, P. S., Permutt, M. A., Matschinsky, F. M., and Herold, K. C. (1998) Familial hyperinsulinism caused by an activating glucokinase mutation. *N. Engl. J. Med.* **338,** 226–230
11. Gloyn, A. L., Noordam, K., Willemsen, M. A., Ellard, S., Lam, W. W., Campbell, I. W., Midgley, P., Shiota, C., Buettger, C., Magnuson, M. A., Matschinsky, F. M., and Hattersley, A. T. (2003) Insights into the biochemical and genetic basis of glucokinase activation from naturally occurring hypoglycemia mutations. *Diabetes* **52,** 2433–2440
12. Cuesta-Muñoz, A. L., Huopio, H., Otonkoski, T., Gomez-Zumaquero, J. M., Näntö-Salonen, K., Rahier, J., López-Enriquez, S., García-Gimeno, M. A., Sanz, P., Soriguer, F. C., and Laakso, M. (2004) Severe persistent hyperinsulinemic hypoglycemia due to a *de novo* glucokinase mutation. *Diabetes* **53,** 2164–2168
13. Grimsby, J., Sarabu, R., Corbett, W. L., Haynes, N. E., Bizzarro, F. T., Coffey, J. W., Guertin, K. R., Hilliard, D. W., Kester, R. F., Mahaney, P. E., Marcus, L., Qi, L., Spence, C. L., Tengi, J., Magnuson, M. A., Chu, C. A., Dvorozniak, M. T., Matschinsky, F. M., and Grippo, J. F. (2003) Allosteric

activators of glucokinase: potential role in diabetes therapy. *Science* **301,** 370–373
14. Kamata, K., Mitsuya, M., Nishimura, T., Eiki, J., and Nagata, Y. (2004) Structural basis for allosteric regulation of the monomeric allosteric enzyme human glucokinase. *Structure* **12,** 429–438
15. Dunten, P., Swain, A., Kammlott, U., Crowther, R., Lukacs, C. M., Levin, W., Reik, L, Grimsby, J., Corbet, W., Magnuson, M. A., Matcshinsky, F. M., and Grippo, J. F. (2004) in *Glucokinase and Glycemic Disease: From Basics to Novel Therapeutics* (*Frontiers in Diabetes*) (Magnuson, M. A., and Matschinsky, F. M., eds) Vol. 16, pp. 145–154, Karger, Basel, *Switzerland*
16. Efanov, A. M., Barrett, D. G., Brenner, M. B., Briggs, S. L., Delaunois, A., Durbin, J. D., Giese, U., Guo, H., Radloff, M., Gil, G. S., Sewing, S., Wang, Y., Weichert, A., Zaliani, A., and Gromada, J. (2005) Novel glucokinase activator modulates pancreatic islet and hepatocyte function. *Endocrinology* **146,** 3696–3701
17. Kester, R. F., Corbett, W. L., Sarabu, R., Mahney, P. E., Haynes, N. E., Guertin, K. R., Bizzarro, F. T., Hilliard, D. W., Qi, L. Tengi, J, Grippo, J. F., Grimsby, J., Marcus, L., Spence, C., Dvorozniak, M., Racha, J., and Wang, K. (2009) in *238th ACS National Meeting, Washington, D. C., Aug. 16–20,* American Chemical Society, Washington, D. C., abstract no. MEDI 5
18. Filipski, K. J., Jones, C. S., Minich, M. L., Wright, S. W., Li, J.-C., Guzman-Perez, A., and Pfefferkorn, J. A. (2010) in *240th ACS National Meeting, Boston, August 22–26,* American Chemical Society, Washington, D. C., abstract no. MEDI 386
19. Pfefferkorn, J. A., Guzmzn-Perez, A., Oates, P. J., Litchfield, J., Aspnes, G., Basak, A., Benbow, J., Berliner, M. A., Bian, J., Choi, C. , Freeman-Cook, K., Corbett, J. W., Didiuk, M., Dunetz, J. R., Filipski, K. J., Hungerford, W. M., Jones, C. S., Karki, K., Ling, A., Li, J., Patel, L., Perreault, C., Risley, H., Saenz, J., Song, W., Tu, M., Aiello, R., Atkinson, K., Barucci, N., Beebe, D., Bourassa, P., Bourbounais, F., Brodeur, A. M., Burbey, R., Chen, J., D'Aquila, T., Derksen, D. R., Haddish-Berhane, N., Huang, C., Landro, J., Lapworth, A. L., MacDougall, M., Perregaux, D., Pettersen, J., Robertson, A., Tan, B., Treadway, J. L., Liu, S., Qiu, X., Knafels, J., Ammirati, M., Song, X., DaSilva-Jardine, P., Liras, S., Sweet, L., and Rolph, T. P. (2011) Designing glucokinase activators with reduced hypoglycemia risk: discovery of *N*,*N*-dimethyl-5-(2-methyl-6-((5-methylpyrazin-2-yl)-carbamoyl-)benzofuran-4-yloxy)pyrimidine-2-carboxamide as a clinical candidate for the treatment of type 2 diabetes mellitus. *Medchemcomm* **2,** 828–839
20. Pfefferkorn, J. A., Guzman-Perez, A., Litchfield, J., Aiello, R., Treadway, J. L., Pettersen, J., Minich, M. L., Filipski, K. J., Jones, C. S., Tu, M., Aspnes, G., Risley, H., Bian, J., Stevens, B. D., Bourassa, P., D'Aquila, T., Baker, L., Barucci, N., Robertson, A. S., Bourbonais, F., Derksen, D. R., Macdougall, M., Cabrera, O., Chen, J., Lapworth, A. L., Landro, J. A., Zavadoski, W. J., Atkinson, K., Haddish-Berhane, N., Tan, B., Yao, L., Kosa, R. E., Varma, M. V., Feng, B., Duignan, D. B., El-Kattan, A., Murdande, S., Liu, S., Ammirati, M., Knafels, J., Dasilva-Jardine, P., Sweet, L., Liras, S., and Rolph, T. P. (2012) Discovery of (*S*)-6-(3-cyclopentyl-2-(4-(trifluoromethyl)-1*H*-imidazol-1-yl)propanamido)nicotinic acid as a hepatoselective glucokinase activator clinical candidate for treating type 2 diabetes mellitus. *J. Med. Chem.* **55,** 1318–1333
21. Bebernitz, G. R., Beaulieu, V., Dale, B. A., Deacon, R., Duttaroy, A., Gao, J., Grondine, M. S., Gupta, R. C., Kakmak, M., Kavana, M., Kirman, L. C., Liang, J., Maniara, W. M., Munshi, S., Nadkarni, S. S., Schuster, H. F., Stams T., St Denny, I., Taslimi, P. M., Vash, B., and Caplan, S. L. (2009) Investigation of functionally liver selective glucokinase activators for the treatment of type 2 diabetes. *J. Med. Chem.* **52,** 6142–6152
22. Petit, P., Antoine, M., Ferry, G., Boutin, J. A., Lagarde, A., Gluais, L., Vincentelli, R., and Vuillard, L. (2011) The active conformation of human glucokinase is not altered by allosteric activators. *Acta Crystallogr. D Biol. Crystallogr.* **67,** 929–935
23. Ricard, J., Meunier, J. C., and Buc, J. (1974) Regulatory behavior of monomeric enzymes. 1. The mnemonical enzyme concept. *Eur. J. Biochem.* **49,** 195–208
24. Ainslie, G. R., Jr., Shill, J. P., and Neet, K. E. (1972) Transients and cooperativity. A slow transition model for relating transients and cooperative kinetics of enzymes. *J. Biol. Chem.* **247,** 7088–7096
25. Buc, J., Ricard, J., and Meunier, J. C. (1977) Enzyme memory. 2. Kinetics and thermodynamics of the slow conformation changes of wheat-germ hexokinase LI. *Eur. J. Biochem.* **80,** 593–601
26. Heredia, V. V., Thomson, J., Nettleton, D., and Sun, S. (2006) Glucose-induced conformational changes in glucokinase mediate allosteric regulation: transient kinetic analysis. *Biochemistry* **45,** 7553–7562
27. Heredia, V. V., Carlson, T. J., Garcia, E., and Sun, S. (2006) Biochemical basis of glucokinase activation and the regulation by glucokinase regulatory protein in naturally occurring mutations. *J. Biol. Chem.* **281,** 40201–40207
28. Lin, S. X., and Neet, K. E. (1990) Demonstration of a slow conformational change in liver glucokinase by fluorescence spectroscopy. *J. Biol. Chem.* **265,** 9670–9675
29. Antoine, M., Boutin, J. A., and Ferry, G. (2009) Binding kinetics of glucose and allosteric activators to human glucokinase reveal multiple conformational states. *Biochemistry* **48,** 5466–5482
30. Larion, M., Salinas, R. K., Bruschweiler-Li, L., Brüschweiler, R., and Miller, B. G. (2010) Direct evidence of conformational heterogeneity in human pancreatic glucokinase from high-resolution nuclear magnetic resonance. *Biochemistry* **49,** 7969–7971
31. Larion, M., and Miller, B. G. (2010) Global fit analysis of glucose binding curves reveals a minimal model for kinetic cooperativity in human glucokinase. *Biochemistry* **49,** 8902–8911
32. Molnes, J., Teigen, K., Aukrust, I., Bjørkhaug, L., Søvik, O., Flatmark, T., and Njølstad, P. R. (2011) Binding of ATP at the active site of human pancreatic glucokinase—nucleotide-induced conformational changes with possible implications for its kinetic cooperativity. *FEBS J.* **278,** 2372–2386
33. Mahalingam, B., Cuesta-Munoz, A., Davis, E. A., Matschinsky, F. M., Harrison, R. W., and Weber, I. T. (1999) Structural model of human glucokinase in complex with glucose and ATP: implications for the mutants that cause hypo- and hyperglycemia. *Diabetes* **46,** 1698–1705
34. Steitz, T. A., Shoham, M., and Bennett, W. S., Jr. (1981) Structural dynamics of yeast hexokinase during catalysis. *Philos. Trans. R. Soc. Lond. B Biol. Sci.* **293,** 43–52
35. Aleshin, A. E., Zeng, C., Bartunik, H. D., Fromm, H. J., and Honzatko, R. B. (1998) Regulation of hexokinase I: crystal structure of recombinant human brain hexokinase complexed with glucose and phosphate. *J. Mol. Biol.* **282,** 345–357
36. Jacques, D. A., and Trewhella, J. (2010) Small-angle scattering for structural biology—Expanding the frontier while avoiding the pitfalls. *Protein Sci.* **19,** 642–657
37. Putnam, C. D., Hammel, M., Hura, G. L., and Tainer, J. A. (2007) Solution scattering (SAXS) combined with crystallography and computation: defining accurate macromolecular structures, conformations and assemblies in solution. *Q. Rev. Biophys.* **40,** 191–285
38. Feigin, L. A., and Svergun, D. I. (1987) in *Structure Analysis by Small-Angle X-ray and Neutron Scattering* (Taylor, G. W., ed) p. 40, Plenum Press, New York
39. Svergun, D. I., Barberato, C., and Koch, M. H. (1995) CRYSOL—a program to evaluate x-ray solution scattering of biological macromolecules from atomic coordinates. *J. Appl. Crystallogr.* **28,** 768–773
40. Krukenberg, K. A., Förster, F., Rice, L. M., Sali, A., and Agard, D. A. (2008) Multiple conformations of *E. coli* Hsp90 in solution: insights into the conformational dynamics of Hsp90. *Structure* **16,** 755–765
41. Otwinowski, Z., and Minor, W. (2001) in *International Tables for Crystallography, Volume F: Macromolecular Crystallography* (Rossmann, M. G., ed) pp. 226–235, Kluwer Academic Publishers, Dordrecht, The Netherlands
42. Vonrhein, C., Flensburg, C., Keller, P., Sharff, A., Smart, O., Paciorek, W., Womack, T., and Bricogne, G. (2011) Data processing and analysis with the autoPROC toolbox. *Acta Crystallogr. D Biol. Crystallogr.* **67**, 293–302
43. Emsley, P., Lohkamp, B., Scott, W. G., and Cowtan, K. (2010) Features and development of Coot. *Acta Crystallogr. D Biol. Crystallogr.* **66**, 486–501
44. Bricogne, G., Blanc, E., Brandl, M., Flensburg, C., Keller, P., Paciorek, P., Roversi, P., Sharff, A., Smart, O., Vonrhein, C., and Womack, T. (2010) *BUSTER*, version 2.9, Global Phasing Ltd., Cambridge, UK
45. Murshudov, G. N., Vagin, A. A., and Dodson, E. J. (1997) Refinement of macromolecular structures by the maximum-likelihood method. *Acta Crystallogr. D Biol. Crystallogr.* **53**, 240–255

46. Yang, L. (2010) *SAXS/WAXS Data Collection at X9. SAXS Workbench*, Brookhaven National Laboratory, New York
47. Kleywegt, G. J., and Jones, T. A. (1997) Detecting folding motifs and similarities in protein structures. *Methods Enzymol.* **277,** 525–545
48. Segal, I. H. (1993) in *Enzyme Kinetics: Behavior and Analysis of Rapid Equilibrium and Steady State Enzyme Systems*, pp. 189–192, Wiley, New York
49. Futamura, M., Hosaka, H., Kadotani, A., Shimazaki, H., Sasaki, K., Ohyama, S., Nishimura, T., Eiki, J., and Nagata, Y. (2006) An allosteric activator of glucokinase impairs the interaction of glucokinase and glucokinase regulatory protein and regulates glucose metabolism. *J. Biol. Chem.* **281,** 37668–37674
50. Zorn, J. A., and Wells, J. A. (2010) Turning enzymes on with small molecules. *Nat. Chem. Biol.* **6,** 179–188
51. DeLano, W. L. (2002) *The PyMOL Molecular Graphics System*, version 1.2r3pre, Schrödinger, LLC, New York

Protein Structure and Folding:

Insights into Mechanism of Glucokinase Activation: OBSERVATION OF MULTIPLE DISTINCT PROTEIN CONFORMATIONS

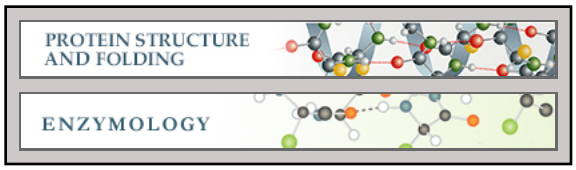

Shenping Liu, Mark J. Ammirati, Xi Song, John D. Knafels, Jeff Zhang, Samantha E. Greasley, Jeffrey A. Pfefferkorn and Xiayang Qiu

J. Biol. Chem. 2012, 287:13598-13610.
doi: 10.1074/jbc.M111.274126 originally published online February 1, 2012